Applied Clay Science 135 (2017) 567–574

Contents lists available at ScienceDirect

Applied Clay Science

journal homepage: www.elsevier.com/locate/clay

Research paper

Clay-biosurfactant materials as functional drug delivery systems: Slowing down effect in the in vitro release of cinnamic acid

Ilaria Calabrese [a], Giulia Gelardi [a,b], Marcello Merli [c], Maria Liria Turco Liveri [a], Luciana Sciascia [c,*]

[a] Dipartimento di Fisica e Chimica, Ed. 17 Università degli Studi di Palermo, 90128 Palermo, Italy
[b] Physical chemistry of building materials, Institute für Baustoffe, ETH Zürich, Schafmattstrasse 6, 8093 Zurich, Switzerland
[c] Dipartimento DiSTeM, Università degli Studi di Palermo, 90126 Palermo, Italy

ARTICLE INFO

Article history:
Received 8 June 2015
Received in revised form 25 October 2016
Accepted 26 October 2016
Available online 3 November 2016

Keywords:
adsorption
Hill isotherm
Cinnammic acid
Montmorillonite
Polyoxyethylene sorbitan monolaurate
Tween 20
Drug delivery systems

ABSTRACT

The main objectives of the present paper were the preparation and characterization of new surfactant-modified clays and the evaluation of their potential applicability as drug delivery systems for the oral administration of the cinnamic acid (CA) drug. The organoclays (OC) were prepared by loading different amounts of the biocompatible nonionic polyoxyethylene sorbitan monolaurate surfactant (Tween20) onto K10 montmorillonite (Mt) clay and characterized through the construction of the adsorption isotherms by means of the spectrophotometric method. The performance of the prepared material was verified by gathering the adsorption isotherms of the cinnamic acid onto the Mt/Tween20 organoclay and by monitoring the release profiles in both simulated gastric (SGF) and intestinal fluids (SIF).

The quantitative analysis of the adsorption isotherms revealed that the uptake of the aromatic component onto both the blank and Tween20-loaded Mt was governed by positive cooperative processes and that the presence of the bio-surfactant enhanced the loading efficiency of the clay.

By relating the raw montmorillonite uptake capability with that of the OC it was assessed that the presence of the bio-surfactant enhanced about 2 times the loading efficiency of the clay. From the XRD characterization of the obtained complexes, the successful intercalation of the drug into the prepared organoclay was demonstrated.

Very useful information was obtained by the in vitro release studies, which showed that the release of the drug from both the clay and organoclay was prolonged in comparison with the pharmacokinetics of the free drug. Besides, the intercalation of the surfactant into the nano-carrier ensured the complete release of the CA after oral drug administration and the kinetics of the release process was strongly dependent on the type of drug formulation used, which means that the CA release can be modulated by properly functionalizing the clay surface.

1. Introduction

Nowadays, the topic of drug administration captures the interest of many scientists and engages them in solving the cogent problem of either over-dosing or under-dosing windows. Considerable efforts have therefore been devoted to the design of appropriate drug delivery systems (DDS) aimed at improving the efficiency and the safety of the product (Kulkarni et al., 2011). In this context clay minerals have been investigated as fundamental constituents of several DDS (Aguzzi et al., 2007; Ambrogi et al., 2012; Calabrese et al., 2013a ; Carretero, 2002; Choy et al., 2007; Iliescu et al., 2011; Nunes et al., 2007; Rodrigues et al., 2013; Viseras et al., 2010; Zheng et al., 2007).

Specifically, montmorillonite (Mt), whose structure consists of two silica tetrahedral sheets sandwiching an edge-shared octahedral sheet of aluminum (T-O-T sheets), attracted a great deal of attention in the research of drug administration (Ambrogi et al., 2012; Carretero, 2002; Cavallaro et al., 2015; Gereli et al., 2006; Lal and Datta, 2012; Lin et al., 2002; Massaro et al., 2015; Wang et al., 2008) because of its noteworthy

List of abbreviations and symbols: CA, Cinnamic acid (cis-3-phenylpropenoic acid); OC, Organoclays; Tween20, Nonionic polyoxyethylene sorbitan monolaurate surfactant; Mt, montmorillonite clay; SGF, simulated gastric fluid; SIF, simulated intestinal fluid; DDS, drug delivery system; FWHM, full width at half-maximum; E(kj m^{-1}), free energy of absorption $E = -(2k)^{-0.5}$; DR equation, Dubinin–Radushkevich equation $\ln C_s = \ln X_m - k\varepsilon^2$; K_F, Freundlich adsorption coefficient; K_L, Langmuir adsorption coefficient; q^m, maximum absorption capacity; K_H, Hill adsorption coefficient; χ^2, Chi square test; *ESS*, sum of squared errors; R^2, coefficient of multiple determination; n, parameter related to the cooperative process; DEM model, Double Exponential Model; $\varepsilon = RT \ln(1 + 1/C_e)$, Polanyi Potentiali; R (kJ mol^{-1} K^{-1}), gas constant; T (K), temperature; C_s (mol g^{-1}), amount of adsorbate per unit weight of adsorbent; X_m (mol g^{-1}), adsorption capacity; C_e (mol dm^{-3}), equilibrium concentration of adsorbate in solution; k (mol^2 k^{-1} J^{-2}), constant related to adsorption energy; A = ε l C, Lambert-Beer law; pV, Pseudo-Voigt function; η, Pseudo-Voigt function mixing parameter; U, V, W, Coefficients of caglioti formula $(FMHM)^2 = (U \tan^2\theta + V\tan\theta + W)^{1/2}$.

* Corresponding author.
E-mail address: luciana.sciascia@unipa.it (L. Sciascia).

http://dx.doi.org/10.1016/j.clay.2016.10.039
0169-1317/

properties including large specific surface area, good adsorption ability, cations exchange capacity, adhesive ability, and drug-carrying and releasing capability.

The already promising features of the clay can be further improved by intercalation with surfactants (Iliescu et al., 2011). The obtained organoclays (OC) exhibit higher organophilic character in comparison with the unmodified clay, i.e., higher uptake ability toward organic substances (Lee and Tiwari, 2012; Shah et al., 2013; Shen, 2004). Moreover, the surfactant functionalization enhances the dispersion stability in aqueous media, which has important implications in adsorption and bioavailability of the drug molecules (Calabrese et al., 2013b; Cavallaro et al., 2014).

In the light of the above considerations, the major objective of the present work lies in the design of an organoclay-based delivery system for the oral administration of the cinnamic acid (cis-3-phenylpropenoic acid) (CA) drug.

This compound was selected because of the very well assessed pharmacologic properties including anti-inflammatory antimicrobial, antimalarial, antioxidant, antidiabetic and anti-cancer activities (Akao et al., 2003; Foti et al., 2004;Wiesner et al., 2001; Zhang and Ji, 1992).

Pharmacokinetics and bioavailability study of CA after oral administration have shown that CA is quickly absorbed, with peak concentrations occurring at 3–10 min after the administration (Chen et al., 2009). This short acting drug requires the use of repeated treatments, which causes the unwanted typical pulsed trend of the plasma concentration of the drug.

The employment of clay and organoclays as nano-carriers for CA delivery system, is here proposed as an efficient alternative to conventional formulations, in order to obtain a slower release of the drug, thus decreasing the number of daily administrations, minimizing the temporal variation of the drug concentration and reducing the side effects.

On the other hand, it should also be taken into account that CA and its phenolic derivatives represent dangerous contaminating agents in wastewaters of agricultural origin (Isidori et al., 2005; Poerschmann et al., 2013). Therefore, the investigation of the adsorption properties of the prepared OC toward this compound, could serve the additional purpose of providing useful information to be exploited in the remediation field.

In the present paper, the organoclays were prepared by loading the biocompatible nonionic polyoxyethylene surfactant (Tween20) onto the K10 montmorillonite (Mt) clay.

The choice of the Tween20 surfactant was prompted by its attested non-toxicity which allows it to be applied in drug delivery systems. The results of some preliminary experiments (Calabrese et al., 2013b) further support this choice because the successful intercalation of the Tween20 onto the clay and the stabilization effect brought about the adsorption of the surfactant on the Mt dispersion, have been demonstrated.

In the first step of the work, the organoclays were prepared and characterized through the construction of the adsorption isotherms. In a second step the adsorption isotherms of the CA compound in both the pristine Mt and the organoclay were studied and the sites of interactions of the clay surface were proposed on the basis of the XRD results. Finally, the release profiles of the CA compound from the prepared hybrids in both simulated gastric (SGF) and intestinal fluids (SIF) pH were investigated.

2. Materials and methods

2.1. Materials

All the reactants, i.e. montmorillonite-K10 (Mt), polyoxyethylene sorbitan monolaurate (Tween20), cinnamic acid (CA), hydrochloric acid (HCl) and sodium hydroxide (NaOH) standard solutions, were purchased from Sigma Aldrich and used as received. Montmorillonite-K10, possesses BET surface area of 220 m^2/g and the following structural formula:

$$(K_{0.25}Na_{0.118}Ca_{0.022})(Al_{1.06}Fe_{0.206}Mg_{0.166})(Si_{7.39}Al_{0.61})O_{20}(OH)_4$$

Although it is known from the literature (Golubeva et al., 2016; Jiang and Zeng, 2003) that Mt of grade K10 contain different impurities (in particular, muscovite and quartz), the choice of this clay mineral was dictated by the extensive literature dealing with the investigation and exploitation for industrial and biomedical applications of K10 Mt/biomolecules complexes. .

Deionized water from reverse osmosis (Elga, model Option 3), having a specific resistance higher than 1 MΩ cm, was used to prepare all solutions.

2.2. Organoclay preparation

Tween20 aqueous stock solutions were prepared by dissolving weighted amounts of the surfactant in an aqueous HCl solution at pH 4.0, previously prepared by proper dilution of the standard 1 M HCl solution.

Mt aqueous dispersion was prepared, according to a procedure previously reported (Sciascia et al., 2011), by crushing the clay mineral in an agate mortar and then mixing 1 g of the powder with 25 mL aqueous HCl solution. The obtained dispersion was stirred for about 2 h before use.

The pH of the aqueous solution/dispersion was measured and, when necessary, the pH was adjusted to pH = 4 by adding microvolumes of HCl or NaOH standard solutions.

The organo-clays were prepared by adding appropriate aliquots of the surfactant solutions to the Mt dispersion at room temperature. The surfactant concentration was changed in the range $1.0–5.0\cdot10^{-3}$ mol dm^{-3} while the amount of Mt was kept constant at 25 mg mL^{-1}. The mixture was stirred for 24 h, then centrifuged 10 min at 8000 rpm by means of a Centra MP4R IEC centrifuge. This way, the supernatant was separated from the solid, which was air dried for 2 days at room temperature and, then, crushed in an agate mortar and employed for XRD characterization. The gathered supernatants were spectrophotometrically analyzed in order to construct the adsorption isotherms. In particular the spectra of the aqueous surfactant solutions were registered in the wavelength range 200–400 nm with a diode-array Analytic Jena S600 spectrophotometer equipped with thermostated compartments for $1 \times 1 \times 5$ cm cuvettes and an appropriate magnetic stirring apparatus.

The Tween 20 aqueous solutions follow the Lambert-Beer law in the concentration range 0.1–6.0 mmol dm^{-3} with a molar absorption coefficients ε of 334 ± 2 dm^3 mol^{-1} cm^{-1} (at λ_{max} = 231.0 nm, R^2 = 0.9998).

Triplicate experiments were performed and the results are reported as the average value of each single measurements.

2.3. Adsorption of the CA into Mt Mt/Tween20 organoclay

The adsorption of the cinnamic acid onto the organoclay prepared by loading the higher surfactant concentration (0.22 mmol g^{-1}), was performed by following the same procedure as for the surfactant adsorption. Adsorption onto the unmodified Mt was also carried out.

Appropriate amounts of stock solution of CA were added to the clay/organoclay aqueous dispersion in order to obtain a CA concentration ranging from $1.0\cdot10^{-5}$ to $9.0\cdot10^{-5}$ mol dm^{-3}.

The mixtures were stirred for 24 h and the resulting products were separated by centrifugation.

The obtained powder was employed for the XRD characterization and for the release tests, while the supernatant was used for the construction of the adsorption isotherm by means of the spectrophotometric method by registering the whole spectrum in the wavelength range 200–400 nm.

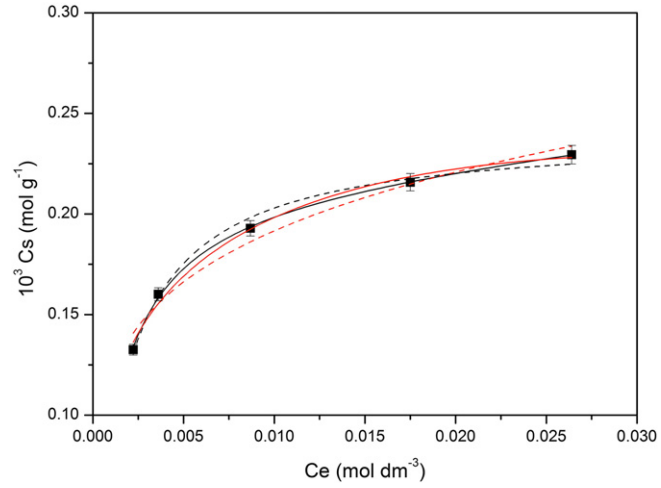

Fig. 1. Adsorption isotherm of Tween20 onto Mt performed at pH = 4.0. Symbols denote experimental points; line corresponds to the fit by Langmuir (black dashed line), Dual Mode Langmuir (black full line), Freundlich (red dashed line) and Dual Mode Freundlich (red full line) models, respectively.

Cinnamic acid aqueous solution followed the Lambert -Beer law in the concentration range 0.003–0.06 mmol dm^{-3} with a molar absorption coefficients ε of 18,500 ± 300 dm^3 mol^{-1} cm^{-1} (at λ_{max} = 270 nm, R^2 = 0.9995).

Experiments were repeated three times and the results, reproducible to within ±2%, are reported as the average value of each single measurements.

2.4. XRD measurements

Powder X-ray diffractometry measurements were performed with a Philips PW 1729 system (Ni filtered Cu Kα radiation, λ = 1.5406 A°, generated at 40 kV and 40 mA, 0.5° beam slit).

Randomly oriented samples were mounted on aluminum plates and the XRD patterns were acquired at room temperature in the range of scattering angles 2θ = 4° ÷ 40°, with step of 0.01°/sec and 1 s counting time.

2.5. Kinetic of CA release

The release of the adsorbed MNE was monitored in media which mimic the physiological pH conditions, i.e. HCl 0.1 M (pH = 1.0) and phosphate buffer (pH = 6.8) at 37.0 °C. These conditions are widely used to reproduce the oral drug administration and the subsequent physiological release (Calabrese et al., 2013a; Hariyadi et al., 2012; Mahkam and A.L., 2015).

The release of CA from both the Mt and Mt/Tween20 support was monitored with an automatic home-made system. 500 mg of the sample were transferred into a dialysis membrane (Spectrapor Dispodialyzer 24,000) and 5 mL of release medium were applied to completely transfer the sample into the membrane. Subsequently, the membrane was put in a glass bottle, containing 100 mL of the release medium (previously thermostated) in an Orbital Shaker at 37.0 °C. The bottle was connected, by means of a peristaltic pump, with a flow cuvette, allocated into an Analytic Jena S600 diode array spectrophotometer which allows to monitor, in real time, the variation of the absorbance of the system as a function of time.

Triplicate release experiments were performed for both drug/clay and drug/organoclay, obtaining a reproducibility of about ±3%.

3. Results and discussion

3.1. Adsorption isotherm of the Tween20 surfactant onto Mt

The adsorption of the Tween20 onto the Mt was carried by changing the surfactant concentration while the amount of Mt was kept constant at 25 g dm^{-3}.

The absorbance values were used to construct the adsorption isotherms (Fig. 1) that were first analyzed by means of the classical Langmuir and Freundlich models, and successively by means of the Dual Mode Langmuir and Dual Mode Freundlich equations.

Langmuir isotherm refers to homogeneous adsorption, where all sites possess equal affinity for the adsorbate while the Freundlich model can be applied to multilayer adsorption, with non-uniform distribution of affinities over the heterogeneous surface (Ringot et al., 2007). As for the Dual Models, two different contributions to the overall sorption process can be recognized: a linear term which is usually (Zhang et al., 2013) attributed to partitioning dominated by hydrophobic interactions and a nonlinear term, related to adsorption-like interactions and characterized from a finite capacity limitation or saturation.

The mathematical expression of the mentioned models, the sorption parameters obtained from the fitting procedure and the related statistical tools (R^2, χ2, ESS) are listed in Table 1. The Dual Mode Langmuir isotherm shows the best values for the statistical indicators.

The linear term could reasonably be attributed to the adsorption of the surfactant onto the in situ prepared organoclay, while the second term is a Langmuir component describing the adsorption processes such as ion exchange or surface adsorption.

The equilibrium data were also treated through the Scatchard plot analysis. The Scatchard equation:

$$\frac{C_s}{C_e} = q_m \cdot K_L - K_L \cdot C_s \quad (1)$$

derives from the mathematical transformations of the classical Langmuir equation which turns out to be very useful and informative for two main reasons. First, by normalizing the C_s value as C_s/C_e the effect of concentration on the shape of Scatchard plot is theoretically eliminated; second, if deviations in the C_s/C_e versus C_s plot from the linearity are observed, they can be ascribed to different binding sites available to the

Table 1
Sorption parameters and selected figures of merit of the different applied models, for the adsorption isotherms of Tween20 onto the Mt.

	Langmuir $C_s = \frac{q^m \cdot K_L \cdot C_e}{1+K_L \cdot C_e}$	Dual Mode Langmuir $C_s = \frac{q^m \cdot K_L \cdot C_e}{1+K_L \cdot C_e} + K' C_e$	Freundich $C_s = K_F \cdot C_e^n$	Dual Mode Freundlich $C_s = K_F \cdot C_e^n + K' C_e$
q_m (mol g^{-1})	(2.4 ± 0.4)·10^{-4}	(2.2 ± 0.5)·10^{-4}		
K_L (dm^3 mol^{-1})	530 ± 40	700 ± 50		
K_F (dm^3 mol^{-1})			(4.9 ± 0.4)·10^{-4}	(9.8 ± 0.3)·10^{-4}
K'(dm^3 mol^{-1})		(9 ± 01)·10^{-4}		(3 ± 1)·10^{-3}
n			0.20 ± 0.02	0.31 ± 0.05
R^2	0.98891	0.99838	0.96778	0.98593
χ^2	3.87·10^{-11}	1.24·10^{-11}	2.95·10^{-10}	1.63·10^{-10}
ESS	1.16·10^{-10}	9.54·10^{-11}	6.73·10^{-10}	8.86·10^{-10}

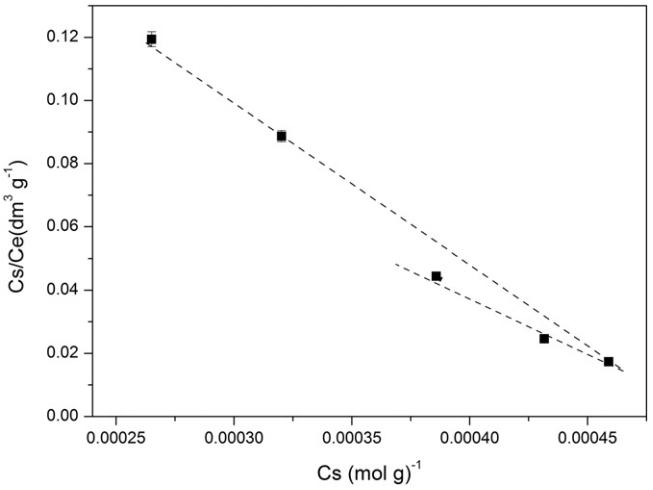

Fig. 2. Scatchard plot for the adsorption of the Tween20 surfactant onto Mt performed at pH = 4.0. Dashed lines are a guide for eyes.

adsorbate, which, in other words, correspond to diverse affinities phenomena. The deviation from the linear trend clearly observable in Fig. 2 supports the existence of different types of site available for the adsorption of the surfactant onto the Mt.

Finally, in order to obtain information about the kind of energy that governs the adsorption process of the bio-surfactant into the clay mineral, the analysis of the equilibrium data was also performed by means of the Dubinin–Radushkevich (DR) equation (Fig. 3):

$$\ln C_s = \ln X_m - k\varepsilon^2 \quad (2)$$

where

$$\varepsilon = \mathrm{RT}\ln(1 + 1/C_e) \quad (3)$$

is the Polanyi Potentiali, R (kJ mol^{-1} K^{-1}) is the gas constant, T (K) is temperature, C_s (mol g^{-1}) is the amount of surfactant adsorbed per unit weight of adsorbent, X_m (mol g^{-1}) is the adsorption capacity, C_e (mol dm^{-3}) is the equilibrium concentration of Tween20 in solution and k (mol^2 k^{-1} J^{-2}) is a constant related to adsorption energy.

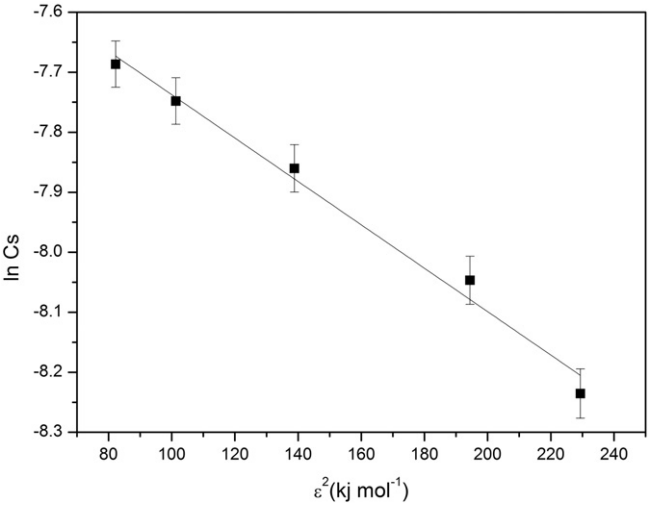

Fig. 3. Dubinin–Radushkevich adsorption isotherms of Tween20 onto Mt. Symbols denote experimental points; line corresponds to the fit by D-R equation.

Table 2
Sorption parameters of the Dubinin–Radushkevich model for the adsorption isotherms of Tween20 onto the Mt.

Dubinin–Radushkevich (Eq. (2))	
X_m (mol g^{-1})	$(6.29 \pm 0.03)\cdot 10^{-4}$
k (mol^2 kJ^{-2})	$(3.6 \pm 0.2)\cdot 10^{-3}$
E(kJ mol^{-1})	11.8 ± 0.6
R^2	0.9838

According to literature (Malik et al., 2005; Singh and Pant, 2004), the magnitude of the mean free energy of adsorption (E), obtained from the value of k by using the equation (Qadeer et al., 1995)

$$E = -(2\,\mathrm{k})^{-0.5} \quad (4)$$

allows to draw the conclusion that chemisorption of the biosurfactant onto Mt occurs.

The obtained values of the sorption parameters are reported in Table 2.

3.2. Adsorption of cinnamic acid onto the organoclays

3.2.1. Preliminary UV–VIS controls

The surfactant modified clays were employed for the adsorption of the cinnamic acid from a test aqueous solutions.

Normalized UV–VIS spectra of the CA aqueous solutions before and after the adsorption onto unmodified Mt and Mt/Tween20 organoclay (Fig. 4A) clearly evidenced that no significant changes neither in the position nor in the band shape occurred.

During the CA loading process, independently of the applied clay, the CA did not undergo to any chemical reaction. By comparing the band intensities (Fig. 4B) it can be noticed that the hydrophobically modified Mt showed a higher loading efficiency with respect to the unmodified one. In fact, the cinnamic acid adsorbed from the aqueous solution by the OC was roughly 60% w/w with respect to the initial concentration while the unmodified Mt was able to uptake only 30% w/w.

In the light of this interesting result, the cinnamic acid/biomodified Mt was further investigated by means of the construction of the adsorption isotherms and the XRD characterization.

3.2.2. Adsorption isotherms of the cinnamic acid onto the organoclay

The adsorption process of the CA onto the prepared Mt/Tween20 complex and, for comparison, onto the unmodified Mt, was performed

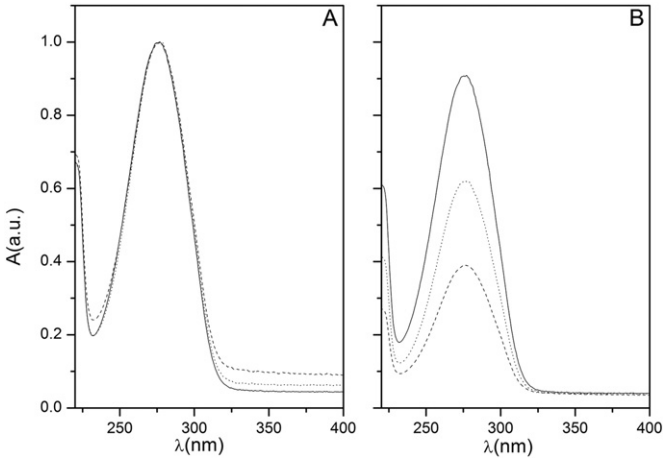

Fig. 4. Normalized (A) and non-normalized (B) UV–VIS spectra of aqueous solution of CA before (solid line) and after the adsorption onto Mt (dotted line) and Mt/Tween20 organoclay (dashed line). The initial concentration of the CA was 0.053 mmol dm^{-3}, pH = 4.

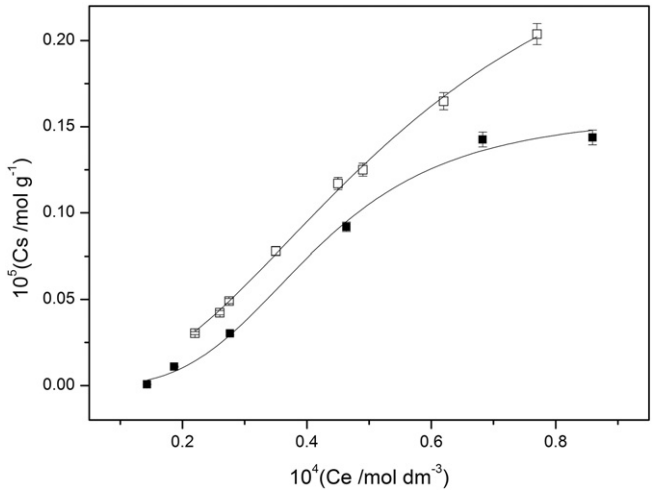

Fig. 5. Adsorption isotherms of cinnamic acid onto the unmodified Mt (■) and onto the prepared organoclay (□). Symbols denote experimental points; line corresponds to the fit by Hill model.

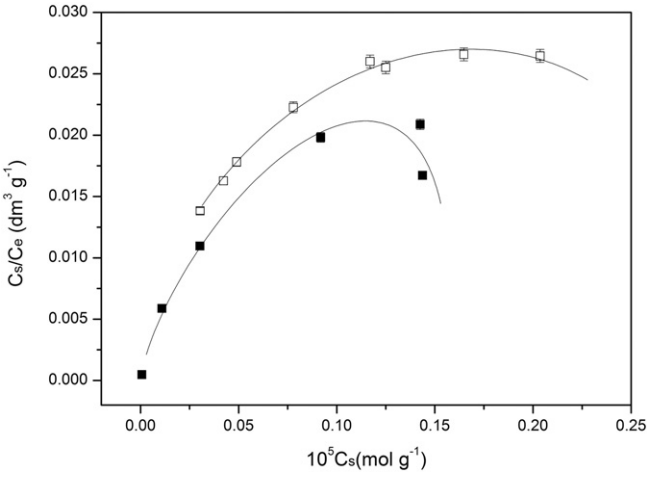

Fig. 6. Scatchard plot of the adsorption of the cinnamic acid onto the prepared organoclay (□) and onto the unmodified Mt (■). Symbols denote experimental points; line corresponds to theoretical curves generated using binding parameters from the fit to the Hill equation.

over a wide range of initial cinnamic acid concentrations keeping constant the amount of Mt. The corresponding adsorption isotherms are shown in Fig. 5.

The adsorption isotherms of cinnamic acid onto both the blank Mt and the organoclay (Fig. 5) follow a sigmoidal curve which, according to Bordbar et al. (1996) is indicative of a positive cooperative process. In other words, the affinity of the CA toward the clay and the organoclay increased on increasing the amount of drug already adsorbed.

Similar results have been recently obtained, for example, in the case of the cellular uptake of boronated porphyrin (Novick et al., 2006).

The data were analyzed by applying, the Freundlich, the Langmuir and the Hill models, and the statistical parameters reported in Table 3 indicate that this last equation represents the most reliable model reproducing the experimental data.

The Hill model assumes that adsorption is a cooperative phenomenon, where the ligand binding ability at one site on the substrate, may influence different binding sites on the same substrate (Ringot et al., 2007).

Table 3
Sorption parameters of Freundlich, Langmuir and Hills models and selected figures of merit for the adsorption isotherms of cinnamic acid onto the unmodified Mt and the surfactant modified clay.

Freundlich		
	Mt	Organoclay
K_F(dm^3 mol^{-1})	0.19 ± 0.01	0.53 ± 0.01
n	1.249 ± 0.008	1.311 ± 0.003
R^2	0.90558	0.97695
χ^2	$3.97\cdot10^{-14}$	$8.92\cdot10^{-15}$
ESS	$1.59\cdot10^{-13}$	$5.35\cdot10^{-14}$
Langmuir		
q_m(mol g^{-1})	$(6.3 \pm 0.6)\cdot10^{-3}$	0.32 ± 0.02
K_L(dm^3 mol^{-1})	2.8 ± 0.3	0.078 ± 0.004
R^2	0.876	0.9205
χ^2	$5.20\cdot10^{-14}$	$3.08\cdot10^{-14}$
ESS	$2.08\cdot10^{-13}$	$1.85\cdot10^{-13}$
Hill		
$Cs = [q_m\cdot(K_H\cdot C_e)^n] / [1 + (K_H\cdot C_e)^n]$ (Eq. (3))		
q^m(mol g^{-1})	$(1.58 \pm 0.08)\cdot10^{-6}$	$(3.0 \pm 0.2)\cdot10^{-6}$
K_H(dm^3 mol^{-1})	$(24 \pm 1)\cdot10^3$	$(18 \pm 1)\cdot10^3$
n	3.6 ± 0.5	2.3 ± 0.1
R^2	0.9934	0.9982
χ^2	$2.77\cdot10^{-15}$	$7.09\cdot10^{-16}$
ESS	$8.30\cdot10^{-15}$	$3.55\cdot10^{-15}$

Interestingly, comparison of the Hill adsorption parameters, reported in Table 3, indicates that the maximum adsorption capacity, q^m, is higher in the case of the organoclay. This proves that the surfactant modified Mt has a higher affinity toward the organic drug than the unmodified clay mineral.

The n parameter values, which are related to the cooperative process, indicates that, in the absence of the surfactant functionalization, the uptake is markedly enhanced by the cinnamic acid content, while

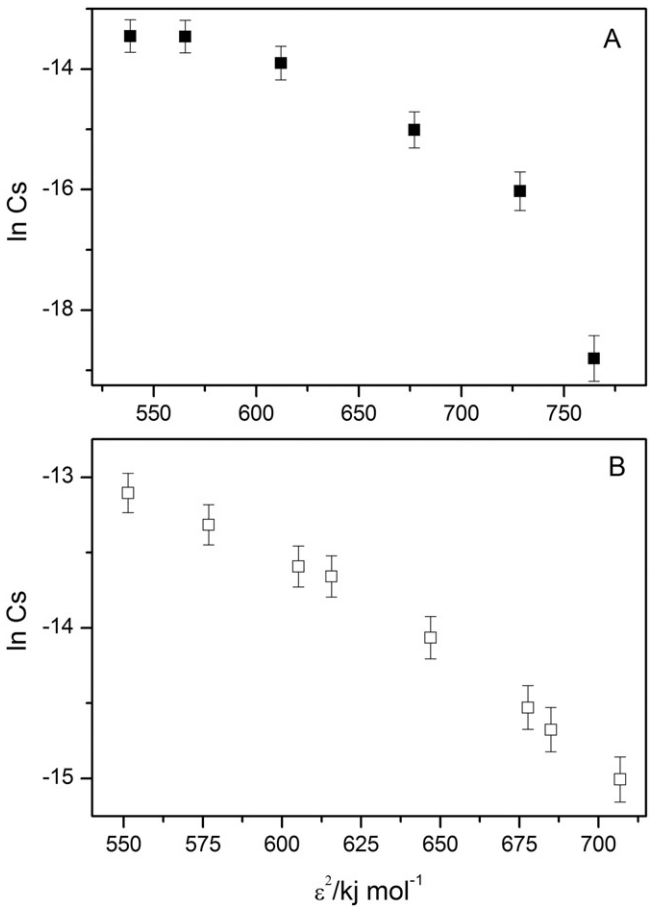

Fig. 7. Dubinin–Radushkevich adsorption isotherms of cinnamic acid onto the prepared organoclay. Symbols denote experimental points.

this effect is less pronounced when the Tween20 surfactant is adsorbed onto the Mt. In other word, the surfactant favors the adsorption of the drug, so that the adsorption is already high also at low CA content.

In order to further support the hypothesis of the positive cooperative interaction, it was verified that the Scatchard plots (Fig. 6) were downward-curved (Bordbar et al., 1996).

Bearing in mind that when the Scatchard curve has this convex shape, the Hill equation is recommended (Bordbar et al., 1996). These curves provide a further confirmation of the reliability of the applied model.

Finally, the Dubinin-Radushkevich approach gave rise to curved plots which means, that, as easily expected, the mean free energy of adsorption changes on changing the amount of sorbate already adsorbed (Fig. 7).

3.2.3. XRD characterization

The adsorption sites of the cinnamic acid onto the blank Mt and the organoclay were investigated by means of XRD measurements (Fig. 8).

In the blank Mt case, the 001 reflection was observed at $2\theta = 5.37°$ ($d = 16.5$ Å). According to the literature (Bromberg et al., 2011; Cui et al., 2008; Calabrese et al., 2016; Bertolino et al., 2016) this reflection has been ascribed to the Mt with interlayer spaces filled with hydrated cations.

The Mt/Tween20 composite exhibited an enlargement of the d-value due to the intercalation in the Mt interlayer space with the surfactant, with the simultaneous expulsion of the water molecules.

The adsorption of the cinnamic acid into the Mt resulted in a sharpening of the reflection near 9.96 Å, corresponding to a slight contraction of the basal spacing with respect to the unmodified Mt, together with the appearance of two overlapping reflections around $2\theta = 5.5°$.

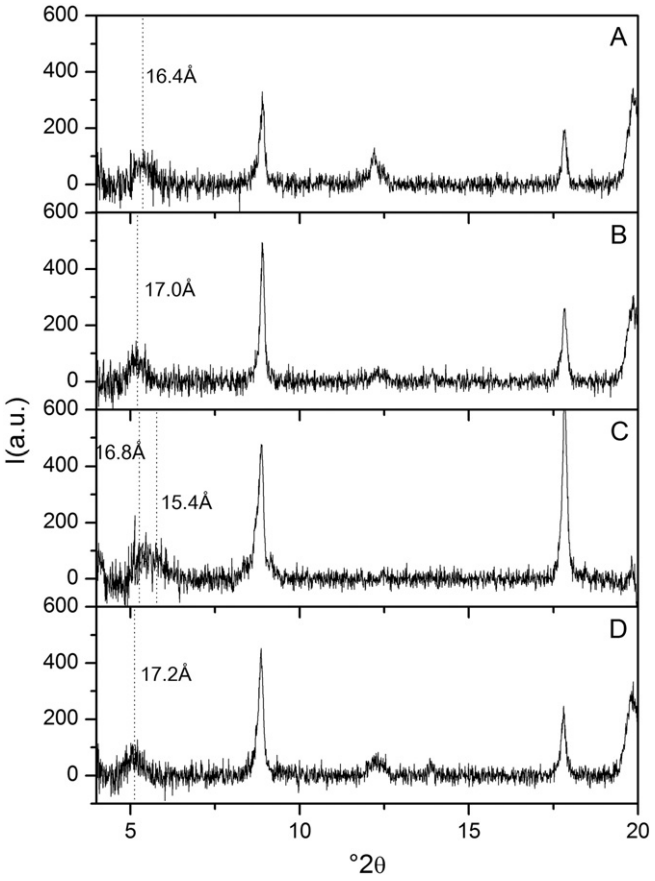

Fig. 8. XRD patterns in the range $4° < 2\theta < 20°$ for (A) Mt, (B) Mt/Tween20, (C) Mt/CA and (D) Mt/Tween20/CA complexes.

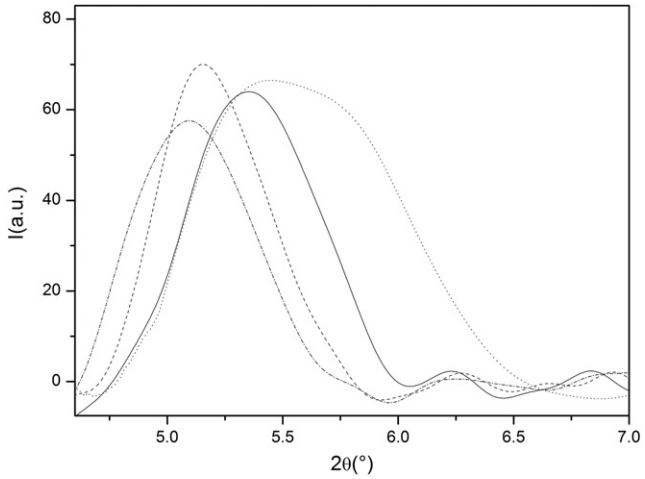

Fig. 9. Superimposition of the calculated XRD patterns in the low angle region for Mt (solid line) Mt/Tween20 (dashed-dotted line), Mt/CA (dotted line) and Mt/Tween20/CA (dashed line).

The lower basal spacing after drug adsorption indicates the successful intercalation of these compounds, which displaced the intercalated water molecules from the interlayer spaces. This phenomenon is typically observed after the absorption of organic species from water solutions onto clays (Rytwo et al., 1996) and has been observed for instance in case of the adsorption of α-2-pralidoxime (PAM) and its zwitterionic oximate form (PAMNa) (Bromberg et al. 2011) or metronidazole (MNE) (Calabrese et al., 2013a) onto K10-Mt.

The presence of the overlapping reflections suggests that the cinnamic acid molecule could be confined in both single or double layers in the interlayer of Mt at the expense of the water content. Either way, the CA intercalation involves positional disorder, as suggested by the high FWHM value of the broad peak at 15.3 Å.

The Mt/Tween20/CA composite, due to the simultaneous intercalation of acid and surfactant, yields an increasing of the d-value up to 17.2 Å.

In order to have a better view of these effects, in Fig. 9 the superimposition of the smoothed XRD patterns in the very low angle region is reported.

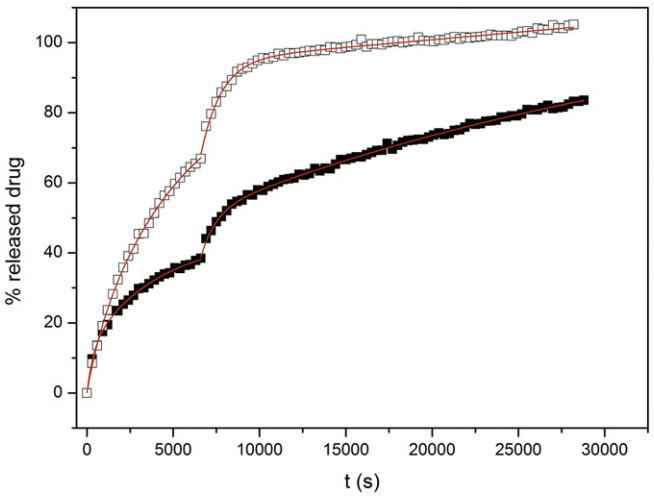

Fig. 10. Kinetics of cinnamic acid release from (■) Mt and (Δ) organoclay. Symbols denote experimental points; line corresponds to the fit by the DEM model.

Table 4
Rate constant values obtained by the application of the DEM model to the release kinetics of cinnamic acid.

	pH 1		pH 6.8	
	Mt	OC	Mt	OC
10^{-4} k_1 (s^{-1})	0.39 ± 0.02	1.37 ± 0.09	0.44 ± 0.06	1.1 ± 0.3
10^{-3} k_2 (s^{-1})	1.2 ± 0.1	0.8 ± 0.2	1.4 ± 0.1	0.99 ± 0.07
R^2	0.9958	0.9989	0.9979	0.9950

3.3. Evaluation of the release capability of the cinnamic acid from the organoclays

The in vitro kinetic release study of the CA from both the Mt and the Tween-modified Mt was undertaken under conditions which mimic oral drug administration and the consequent physiological release.

The obtained cumulative release profiles are reported in Fig. 10.

The kinetic behavior of the release process was strongly dependent on the type of drug formulation used, which means that the cinnamic acid release can be modulated by properly functionalizing the Mt surface. Indeed, comparison of the trends obtained for the two types of formulations revealed that, as for the *organoclay*, a conspicuous amount of cinnamic acid, about 70%, is released at pH = 1 and after 6 h almost the 100% of the drug is present in the buffered medium at pH = 6.8 as free drug. Differently, a lower amount of the cinnamic acid, about 40%, loaded into the unmodified Mt is released at pH = 1 within the first 2 h of incubation, and on passing time (6 h) the amount of released drug increased at pH = 6.8 till a value of about 80% of released drug.

Therefore, the intercalation of the surfactant into the nano-carrier ensured the complete release of the cinnamic acid after oral drug administration.

The quantitative analysis of the kinetic data, revealed the release kinetics, for both the pH values investigated, followed a Double Exponential Model (DEM) which indicates the occurrence of two parallel release steps (Qiu et al., 2009).

This behavior can be interpreted by considering that the drug release is due to the breakage of either the interactions between drugs molecules (drug-drug interaction) or those between clay/organoclay and drug molecules.

The kinetic rate constant values obtained by the application of the DEM model (Table 4) indicates the presence of the surfactant onto the Mt exerted a significant effect on the process associated with the lower rate constant value (k_1).

Indeed, as for this reaction step, which can be reasonable associated to the release of the CA from the interlayer spaces of the hybrids (breakage of the drug-clay/organoclay interaction) the drug release from the OC was faster than that from the unmodified Mt.

As for the faster reaction step (breakage of the drug-drug interaction) the effect of the presence of the surfactant is obviously less effective, since the Tween20 molecules are not involved in the hydrophobic interactions between drug molecules.

Comparison with the pharmacokinetic studies of the free cinamic acid reported in literature (Chen et al., 2009) reveals a significant slowing down effect in the release of the encased drug.

The low release e rate represents an accomplishment of the prefixed target, since it implies that CA therapy should not require repeated treatments, thus avoiding unwanted pulsed trend of the drug concentration in the plasma.

4. Conclusions

Hybrid materials based on the non-ionic surfactant Tween20 and Mt were prepared and characterized through the construction of the adsorption isotherms and XRD measurement. The performances of the new prepared material were thus verified by employing them for the adsorption and release of the cinnamic acid. A comparison with the unmodified Mt revealed that the hybrid complexes proved much effective in the adsorption of the drug.

The in vitro release studies revealed that the encapsulation of the drug into both clays and organoclays allowed for a prolonged release drug, compared with the release of the free drug., which is an important achievement of an efficient drug delivery system.

Furthermore the intercalation of the surfactant into the hybrid nanocarrier, not only allowed to load an higher amount of drug, in comparison with the raw clay, but it also ensured the complete release of the CA after oral drug administration. These results imply that the prepared OC might be considered as promising materials for the design of novel drug delivery systems for the CA administration.

Acknowledgements

The authors gratefully acknowledge the financial support provided by the MIUR (PRIN grant 2010EARRRZ_003) and local funds from University of Palermo (MURST ex 60% grant).

References

Aguzzi, C., Cerezo, P., Viseras, C., Caramella, C., 2007. Use of clays as drug delivery systems: possibilities and limitations. Appl. Clay Sci. 36, 22–36.
Akao, Y., Maruyama, H., Matsumoto, K., Ohguchi, K., Nishizawa, K., Sakamoto, T., Araki, Y., Mishima, S., Nozawa, Y., 2003. Cell growth inhibitory effect of cinnamic acid derivatives from propolis on human tumor cell lines. Biol. Pharm. Bull. 26, 1057–1059.
Ambrogi, V., Latterini, L., Nocchetti, M., Pagano, C., Ricci, M., 2012. Montmorillonite as an agent for drug photostability. J. Mater. Chem. 22, 22743–22749.
Bertolino, V., Cavallaro, G., Lazzara, G., Merli, M., Milioto, S., Parisi, F., Sciascia, L., 2016. Effect of the biopolymer charge and the nanoclay morphology on nanocomposite materials. Ind. Eng. Chem. Res. 55, 7373–7380.
Bordbar, A.K., Saboury, A.A., Moosavi-Movahedi, A.A., 1996. The shapes of Scatchard plots for systems with two sets of binding sites. Biochem. Educ. 24, 172–175.
Bromberg, L., Straut, C.M., Centrone, A., Wilusz, E., Hatton, T.A., 2011. Montmorillonite functionalized with pralidoxime as a material for chemical protection against organophosphorous compounds. Appl. Mater. Interfaces 3, 1479.
Calabrese, I., Cavallaro, G., Scialabba, C., Licciardi, M., Merli, M., Sciascia, L., Turco Liveri, M.L., 2013a. Montmorillonite nanodevices for the colon metronidazole delivery. Int. J. Pharm. 457, 224–236 Special Section: Formulating Better Medicines for Children.
Calabrese, I., Gelardi, G., Merli, M., Rytwo, G., Sciascia, L., Liveri, M.L.T., 2013b. New Tailor-Made Bio-Organoclays for the Remediation of Olive Mill Waste Water, in: 2nd International Conference on Competitive Materials and Technological Processes (ic-Cmtp2). Iop Publishing Ltd, Bristol.
Calabrese, I., Cavallaro, G., Lazzara, G., Merli, M., Sciascia, L., Turco Liveri, M.L., 2016. Preparation and characterization of bio-organoclays using nonionic surfactant. Adsorption 22, 105–116.
Carretero, M.I., 2002. Clay minerals and their beneficial effects upon human health. A review. Appl. Clay Sci. 21, 155–163.
Cavallaro, G., Lazzara, G., Milioto, S., Parisi, F., Sanzillo, V., 2014. Modified halloysite nanotubes: nanoarchitectures for enhancing the capture of oils from vapor and liquid phases. ACS Appl. Mater. Interfaces 6, 606–612.
Cavallaro, G., Lazzara, G., Massaro, M., Milioto, S., Noto, R., Parisi, F., Riela, S., 2015. Biocompatible poly(*N*-isopropylacrylamide)-halloysite nanotubes for thermoresponsive curcumin release. J. Phys. Chem. C 119, 8944–8951.
Chen, Y., Ma, Y., Ma, W., 2009. Pharmacokinetics and bioavailability of cinnamic acid after oral administration of Ramulus Cinnamomi in rats. Eur. J. Drug Metab. Pharmacokinet. 34, 51–56.
Choy, J.-H., Choi, S.-J., Oh, J.-M., Park, T., 2007. Clay minerals and layered double hydroxides for novel biological applications. Appl. Clay Sci. 36, 122–132.
Cui, L., Tarte, N.H., Woo, S.I., 2008. Effects of modified clay on the morphology and properties of pmma/clay nanocomposites synthesized by in situ. Polym. Macromol. 41, 4268–4274.
Foti, M.C., Daquino, C., Geraci, C., 2004. Electron-transfer reaction of cinnamic acids and their methyl esters with the DPPH(*) radical in alcoholic solutions. J. Org. Chem. 69, 2309–2314.
Gereli, G., Seki, Y., Murat Kuşoğlu, İ., Yurdakoç, K., 2006. Equilibrium and kinetics for the sorption of promethazine hydrochloride onto K10 montmorillonite. J. Colloid Interface Sci. 299, 155–162.
Golubeva, O.Y., Shamova, O.V., Yakovlev, A.V., Zharkova, M.S., 2016. Synthesis and study of the biologically active lysozyme–silver nanoparticles–montmorillonite K10 complexes. Glas. Phys. Chem. 42, 87–94.
Hariyadi, D.M., Wang, Y., Lin, S.C.-Y., Bostrom, T., Bhandari, B., Coombes, A.G.A., 2012. Novel alginate gel microspheres produced by impinging aerosols for oral delivery of proteins. J. Microencapsul. 29, 250–261.
Iliescu, R.I., Andronescu, E., Voicu, G., Ficai, A., Covaliu, C.I., 2011. Hybrid materials based on montmorillonite and citostatic drugs: preparation and characterization. Appl. Clay Sci. 52, 62–68.

Isidori, M., Lavorgna, M., Nardelli, A., Parrella, A., 2005. Model study on the effect of 15 phenolic olive mill wastewater constituents on seed germination and Vibrio fischeri metabolism. J. Agric. Food Chem. 53, 8414–8417.
Jiang, J.Q., Zeng, Z., 2003. Comparison of modified montmorillonite adsorbents: part II. The effects of thetype of raw clays and modification conditions on the adsorption performance. Chemosphere 53, 53–62.
Kulkarni, P.R., Yadav, J.D., Vaidya, K.A., 2011. Liposomes: a novel drug delivery system. Int. J. Curr. Pharm. Res. 3, 10–18.
Lal, S., Datta, M., 2012. In vitro prolonged gastric residence and sustained release of atenolol using novel clay polymer nanocomposite. Appl. Clay Sci. 114, 412–421.
Lee, S., Tiwari, D., 2012. Organo and inorgano-organo-modified clays in the remediation of aqueous solutions: an overview. Appl. Clay Sci. 59–60, 84–102.
Lin, F.H., Lee, Y.H., Jian, C.H., Wong, J.-M., Shieh, M.-J., Wang, C.-Y., 2002. A study of purified montmorillonite intercalated with 5-fluorouracil as drug carrier. Biomaterials 23, 1981–1987.
Malik, U.R., Hasany, S.M., Subhani, M.S., 2005. Sorptive potential of sunflower stem for Cr(III) ions from aqueous solutions and its kinetic and thermodynamic profile. Talanta 66, 166–173.
Massaro, M., Colletti, C.G., Noto, R., Riela, S., Poma, P., Guernelli, S., Parisi, F., Milioto, S., Lazzara, G., 2015. Pharmaceutical properties of supramolecular assembly of co-loaded cardanol/triazole-halloysite systems. Int. J. Pharm. 478, 476–485.
Mahkam, M., A.L., 2015. Preparation of montmorillonite-pH-sensitive positive charges nanocomposites as a drug delivery system. Int. J. Polym. Mater. 64, 32–37.
Novick, S., Laster, B., Quastel, M.R., 2006. Positive cooperativity in the cellular uptake of a boronated porphyrin. Int. J. Biochem. Cell Biol. 38, 1374–1381.
Nunes, C.D., Vaz, P.D., Fernandes, A.C., Ferreira, P., Romão, C.C., Calhorda, M.J., 2007. Loading and delivery of sertraline using inorganic micro and mesoporous materials. Eur. J. Pharm. Biopharm. 66, 357–365.
Poerschmann, J., Weiner, B., Baskyr, I., 2013. Organic compounds in olive mill wastewater and in solutions resulting from hydrothermal carbonization of the wastewater. Chemosphere 92, 1472–1482.
Qadeer, R., Hanif, J., Khan, M., Saleem, M., 1995. Uptake of uranium ions by molecular sieve. Radiochim. Acta 68, 197–201.
Qiu, H., Lv, L., Pan, B., Zhang, Q., Zhang, W., Zhang, Q., 2009. Critical review in adsorption kinetic models. J. Zhejiang Univ. Sci. A 10, 716–724.
Ringot, D., Lerzy, B., Chaplain, K., Bonhoure, J.-P., Auclair, E., Larondelle, Y., 2007. In vitro biosorption of ochratoxin A on the yeast industry by-products: comparison of isotherm models. Bioresour. Technol. 98, 1812–1821.
Rodrigues, L.A.d.S., Figueiras, A., Veiga, F., de Freitas, R.M., Nunes, L.C.C., da Silva Filho, E.C., da Silva Leite, C.M., 2013. The systems containing clays and clay minerals from modified drug release: a review. Colloids Surf. B Biointerfaces 103, 642–651.
Rytwo, G., Nir, S., Margulies, L., 1996. A model for adsorption of divalent organic cations to montmorillonite. J. Colloid Interface Sci. 181, 551–560.
Sciascia, L., Turco Liveri, M.L., Merli, M., 2011. Kinetic and equilibrium studies for the adsorption of acid nucleic bases onto K10 montmorillonite. Appl. Clay Sci. 53, 657–668.
Shah, K.J., Mishra, M.K., Shukla, A.D., Imae, T., Shah, D.O., 2013. Controlling wettability and hydrophobicity of organoclays modified with quaternary ammonium surfactants. J. Colloid Interface Sci. 407, 493–499.
Shen, Y.-H., 2004. Phenol sorption by organoclays having different charge characteristics. Colloids Surf. Physicochem. Eng. Asp. 232, 143–149.
Singh, T.S., Pant, K.K., 2004. Equilibrium, kinetics and thermodynamic studies for adsorption of As(III) on activated alumina. Sep. Purif. Technol. 36, 139–147.
Viseras, C., Cerezo, P., Sanchez, R., Salcedo, I., Aguzzi, C., 2010. Current challenges in clay minerals for drug delivery. Appl. Clay Sci. 48, 291–295.
Wang, X., Du, Y., Luo, J., 2008. Biopolymer/montmorillonite nanocomposite: preparation, drug-controlled release property and cytotoxicity. Nanotechnology 19, 065707.
Wiesner, J., Mitsch, A., Wissner, P., Jomaa, H., Schlitzer, M., 2001. Structure-activity relationships of novel anti-malarial agents. Part 2: cinnamic acid derivatives. Bioorg. Med. Chem. Lett. 11, 423–424.
Zhang, L.P., Ji, Z.Z., 1992. Synthesis, antiinflammatory and anticancer activity of cinnamic acids, their derivatives and analogues. Yao Xue Xue Bao 27, 817–823.
Zhang, Q., Yang, C., Huang, W., Dang, Z., Shu, X., 2013. Sorption of tylosin on clay minerals. Chemosphere 93, 2180–2186.
Zheng, J.P., Luan, L., Wang, H.Y., Xi, L.F., Yao, K.D., 2007. Study on ibuprofen/montmorillonite intercalation composites as drug release system. Appl. Clay Sci. 36, 297–301.